Doping Dependence on Superconducting Transition in High-Temperature Superconductor $La_{2-x}Sr_xCuO_4$

Anita Kumari Maliyan
Dept. of Physics
SGRR (PG) College, Dehradun
Email: anitasgrrpg.ddun@gmail.com

Sanjeev K. Verma
Dept. of Physics
IILM University,
Greater Noida

Reference to this paper should be made as follows:
Received: 16-12-2025
Approved: 26-12-25

Anita Kumari Maliyan
Sanjeev K. Verma

Doping Dependence on Superconducting Transition in High-Temperature Superconductor $La_{2-x}Sr_xCuO_4$

Voyager: Vol. XVI, 2025
Article No. 15,
Pg. 132-147

Similarity Check: 10%

Online available at:
https://anubooks.com/journal-volume/voyager-vol-xvi-2025

DOI: *https://doi.org/10.31995/voyager.2025.v16.015*

Abstract

The doping dependence of transition temperature has been perceived since the discovery of a high-temperature superconductor by Bednorz and Müller. The compound $La_{2-x}Sr_xCuO_4$ with x=0.03 to 0.15 of Sr replacing La, is orthorhombic at low temperature and low Sr contents and is tetragonal otherwise. The critical temperature T_c in $La_{2-x}Sr_xCuO_4$ has an arc-shaped or hemisphere-shaped concentration x dependence and a maximum of about 30 K at the doping concentration of x= 0.15 and decreases on both sides in the range of $0.05 \leq x \leq 0.25$. The present work is dedicated to the study of various scattering phenomena and the doping dependence of Sr on HTS $La_{2-x}Sr_xCuO_4$ for x=0.02, 0.04 (for the non-superconducting range) and for x= 0.12, 0.15 (for the superconducting range). This offers an asset to understand the basic phenomenon that causes superconductivity in these materials and to develop the appropriate preparation methods so that these can be exploited for a wide range of applications.

Keywords

Antiferromagnetic; High temperature superconductors; Doping; ARPES https://doi.org/10.31995/voyager.2025.v16.015

1. Introduction

Even after more than 35 years of its discovery, the interest in high-temperature superconductivity is still going strong due to its great potential for applications. This class of materials not only shows high-temperature superconductivity but also shows properties that are different from classical superconductors. The first high-temperature superconductor (HTS) discovered in 1986 was a ceramic $La_{2-x}Ba_xCuO_4$ (LBCO) with transition temperature T_c of 35 K [1]. The parent compound La_2CuO_4 is antiferromagnetic in nature with Neel's temperature, T_N = 270 K and must be doped, generally with an alkaline earth element like Sr or Ba, to exhibit pronounced superconducting properties. The doping dependence of transition temperature has been perceived since the discovery of a high-temperature superconductor by Bednorz and Müller. The compound $La_{2-x}Sr_xCuO_4$ with x=0.03 to 0.15 of Sr replacing La, is orthorhombic at low temperature and low Sr contents and is tetragonal otherwise. The critical temperature T_c in $La_{2-x}Sr_xCuO_4$ has an arc-shaped or hemisphere-shaped concentration x dependence and a maximum of about 30 K at the doping concentration of x= 0.15 and decreases on both sides in the range of $0.05 \leq x \leq 0.25$ [2]. There are many approaches to evaluate thermal conductivity, with a tremendous rise in the computational power and the availability of popular methods like Density Functional Theory (DFT) to deal with the many-body problem, one can combine DFT with a variety of computer codes especially designed for the evaluation of the transport properties. This route is gaining much popularity, particularly for the purpose of finding potential thermo-electric materials.

The other route, e.g. model calculations using the Quantum Dynamical approach, is more involved analytically and is quite challenging too. This seems to be a less trodden path, nevertheless, this too has its own beauty. Hence both the approaches stand out on their own. The present work deals with the evaluation of the thermal conductivity and scattering phenomenon of $La_{2-x}Sr_xCuO_4$ at different doping levels using the Quantum Dynamical approach. The formulation has been applied to single crystals which help unfurl the anisotropicity of the layered cuprates. The results yield good agreement with the available experimental data and lend an insight into the scattering processes [3,4,5,6,7] has already been published on the thermal properties of LSCO high temperature superconductor.

In view of the availability of experimental data for thermal conductivity for the doped $La_{2-x}Sr_xCuO_4$, and in the superconducting as well as non-superconducting range, the LSCO system offers an excellent testbed for the theoretical evaluation of its anisotropic thermal conductivity.

The following section is devoted to a brief introduction of the HTS $La_{2-x}Sr_xCuO_4$, various scattering phenomena for in-plane and cross-plane are briefly discussed. Also, efforts have been made to analyse the effect of Sr doping concentration on the superconducting transition of $La_{2-x}Sr_xCuO_4$.

2. Formulation of the Problem

2.1 The High Temperature Superconductor $La_{2-x}Sr_xCuO_4$

The $La_{2-x}Sr_xCuO_4$ or LSCO, has a layered structure. The unit cell for the parent compound La_2CuO_4 (LCO), is shown in Figure 1. The advancement of layers in the unit cell along the c-axis for the parent compound La_2CuO_4 can be represented by CuO_2- LaO - LaO - CuO_2 - LaO - LaO - CuO_2. It has equally spaced CuO_2 layers stacked one above the other. The formation of pairons or the flow of supercurrent takes place in these CuO_2 conduction layers. These conduction layers are bound together in the structure by the -LaO - LaO - binding layers[8].

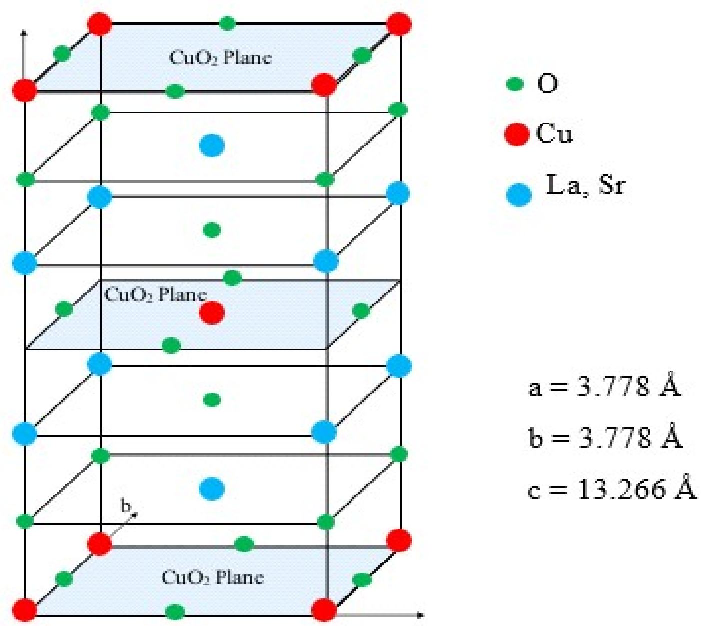

Figure-1: Unit cell of $La_{2-x}Sr_xCuO_4$[9]

In the conduction layers i.e. copper-oxide (CuO_2) planes, each copper ion (Cu^{2+}) is surrounded by four oxygen ions (O^{2-}). The copper is octahedrally coordinated with oxygen, however, the distance (= 1.9 Å) from Copper to Oxygen in the CuO_2 planes is much less than the vertical distance of 2.4 Å from Copper to the apical oxygen [8]. This leads to the anisotropic behaviour in heat transport in LSCO. The binding layers are also called as charge reservoir layers [10] as they provide charge to the conduction layer. There is a charge transfer, to and from the conduction layers (CuO_2), which is influenced by doping near the metal-insulator phase boundary (Figure-2). Also, the magnitude of various physical properties and the nature of the compound change with the different doping concentrations. The Phase Diagram of the system $La_{2-x}Sr_xCuO_4$ or LSCO, is illustrated in Figure -2.

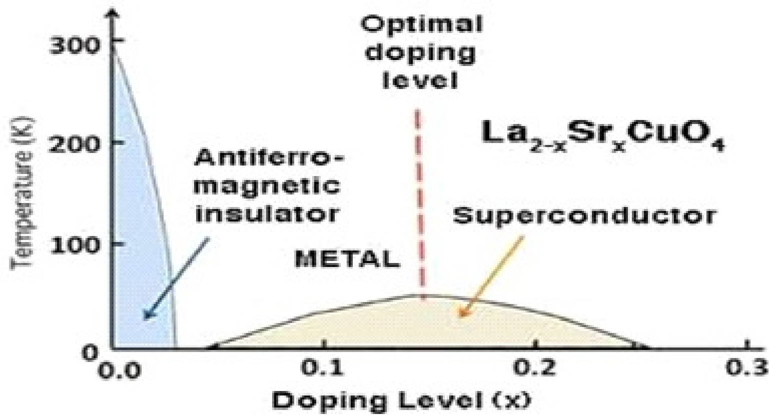

Figure-2: Phase diagram for $La_{2-x}Sr_xCuO_4$[2]

As a chemical compound, one may express the parent compound as $(La_2)^{3+}$ $(Cu)^{2+}$ $(O_4)^{2"}$ and it is antiferromagnetic in nature with Neel temperature, $T_N \sim 270$ K [4,11,12]. Now, when some La^{3+} ions are replaced by Sr^{2+} doping, one can either have a Cu^{3+}, or an O^{1-} ion corresponding to each Sr^{2+} ion, i.e. a hole is introduced or doped into the LSCO. Hence, the addition of a Sr^{2+} ion, replacing a La^{3+}, introduces a hole in the CuO_2 planes. The Sr concentration in LSCO can be regarded as the hole concentration per Cu atom for pairon formation in the CuO_2 planes. This introduction of holes via Sr doping replacing a La^{3+}, helps in explaining conduction in the CuO_2 planes and gives rise to hole-doped high-temperature superconductor LSCO in a suitable range of doping as shown in the phase diagram. So, LCO must be doped, generally with an alkaline earth element like Sr or Ba, to exhibit pronounced superconducting properties. The compound $La_{2-x}Sr_xCuO_4$ with x = 0.03 to 0.15, is orthorhombic at low temperature and is tetragonal otherwise [8]. The critical temperature T_c in $La_{2-x}Sr_xCuO_4$ has an arc or hemisphere-shaped dependence on doping concentration x and the maximum T_c occurs at ~37 K [9], at the optimum doping concentration of $x = 0.15$ and decreases on both sides in the range $\sim 0.05 \leq x \leq 0.25$ (Figure-2).

A strong superexchange interaction between copper spins, via oxygen ions, gives rise to the long-range antiferromagnetic order in the parent compound La_2CuO_4 with Neel

Temperature around 270 K [10,11]. Although, this long-range antiferromagnetic order is troubled on doping Sr by replacing some La ions, for a certain range of doping as stated above, the compound becomes superconducting in nature.

2.2 Scattering Rates and Thermal Conductivity

The problem of heat transport in layered $La_{2-x}Sr_xCuO_4$ has been examined in the framework along the CuO_2 plane and across the CuO_2 plane at different doping concentration x of Sr for the non-superconducting range (x= 0.02 and 0.04) and superconducting range (x= 0.12 and 0.15) by utilizing the modified Callaway model of thermal conductivity based on relaxation time (line-width) approximation.

Employing the many-body quantum dynamical theory, the inverse relaxation time, taken in terms of line-width for various scattering events such as combined boundary, impurity or defects, interference etc. has been studied for superconducting $La_{1.88}Sr_{0.12}CuO_4$, also the expressions for thermal conductivity in the frame of in-plane and cross-plane have been obtained for both non-superconducting and superconducting ranges.

The thermal conductivitykof a crystal can be expressed as [13]:

$$\kappa = \sum_i \left(\frac{k_B}{2\pi^2 v}\right)\left(\beta^2\hbar^2\right)\int_0^{\omega_D} \tau_i \frac{\omega_i^4 e^{\beta\hbar\omega_i}}{\left(e^{\beta\hbar\omega_i}-1\right)^2} d\omega_i; \quad i \equiv ab, c \tag{1}$$

The $\tau^{-1}(\omega)$ is related to the line-width $\Gamma(\omega)$ as

$$\tau^{-1}(\omega) = \Gamma(\omega) \tag{2}$$

$$\tau^{-1}(\omega) = \sum_i \tau_i^{-1}(\omega) = \Gamma(\omega), \tag{3}$$

where i represents various scattering processes. Hence the expanded form of is $\tau^{-1}(\omega)$ is

$$\tau_k^{-1}(\omega) \approx \tau_{CB}^{-1}(\omega) + \Gamma_k^{D}(\omega) + \Gamma_k^{3A}(\omega) + \Gamma_k^{AD}(\omega) + \Gamma_k^{ep}(\omega) + \tau_R^{-1}(\omega) \tag{4}$$

where i represents various scattering processes. Hence the expanded form of is $\tau^{-1}(\omega)$ is detailed description of various terms used in the above equations is present in the reference [14]. The phonon frequency line width $\Gamma(\omega)$ plays an important role in examining the thermal properties of HTS since $\Gamma(\omega) = \tau^{-1}(\omega)$ and the relaxation time $\tau^{-1}(\omega)$ influences the k directly through equation [13]. $\tau^{-1}(\omega)$ represents the scattering rate and has significant contribution from a large number of collision processes [15,16,17] which can be expressed as combined boundary scattering, defect or impurity scattering, phonon-phonon scattering, interference scattering, electron-phonon scattering and resonance scattering.

3. Results and Discussions

As per the phase diagram (Figure-2), as the doping of Sr is done to replace a few La atoms, the material is still non-superconducting for very low doping, and then becomes superconducting for a certain range of doping. Hence, the κ has been studied for both, the non-superconducting $La_{2-x}Sr_xCuO_4$ (x =0.02 and 0.04) and the superconducting $La_{2-x}Sr_xCuO_4$ (x = 0.12 and 0.15). Also, the phenomenon of scattering processes for in-plane and cross-plane superconducting $La_{2-x}Sr_xCuO_4$ (x = 0.12) has been explored.

3.1 The Inverse Relaxation Time or Line-widths for Various Scattering Processes

Prior to presenting the results for the thermal conductivity, first the scattering rates have been studied. The results for inverse relaxation time (or alternatively the line width) have been presented for various scattering processes. For this subsection, the superconducting LSCO with x = 0.12 has been used as a representative material. It may be noted that since pairons don't exchange thermal energy with the phonons [18], the trend is expected to be somewhat different for doping concentrations x = 0.02, 0.04 which fall in the non-superconducting regime.

3.1.1 for Modified Combined Boundary Scattering

At fairly low temperature, the long-wavelength phonons (low-frequency phonons) are predominant and start immigrating. These phonons are scattered mainly from the crystal boundaries. For various reasons stated in the last chapter, the actual length for the scattering is different from the physical dimensions of the crystal [19]. The phenomenon of combined boundary scattering is generally observed at very low temperatures and for an anisotropic scenario, it may be expressed as, $\tau_{CB}^{-1} = \sum_j v_j / L_j(B)$ with v_j as the phonon velocity and $L_j(B)$ is the modified Casimir length along *j*- axes and $L_j(B) = 1.22 B_j(I)\left(l_1 l_2\right)^{1/2}$ where $B_j(I)$ internal boundary parameter, l_1, l_2 are the cross-sections of the specimen. This scattering is effectively temperature independent, whereas as seen ahead, all others are temperature dependent and start building up with the rise in temperature. Hence this scattering plays a significant role at very low temperatures. This would also be applicable to other LSCO members studied in this paper.

3.1.2 for Defect Scattering

The presence of isotopic point impurities or defects offers noticeable resistance to the phonons transporting the thermal energy. The corresponding phonon line-width (inverse relaxation time) for LSCO ($x = 0.12$) has been examined. The variation of defect scattering rates (or inverse relaxation time) with Figure-3 shows the trend of inverse relaxation time for defect scattering with reduced frequency ($y = h\omega/k_BT$) at the transition temperature, and below (at 20 K) and above (at 60 K) it. The scattering rate at any given frequency is larger at $T \geq T_c$, and decreases as T decreases to Tc and then a further drop in scattering rate is observed for T ≤ T_c. The same trend has been observed for all the scattering processes for superconducting LSCO.

Figure-3 shows the trends of inverse relaxation time for defect scattering with reduced frequency (y = hω/k_BT) at transition temperature and below (at 20 K) and above (at 60 K) it. The variation of inverse relaxation time for 20 K is less steep for this scattering for both in-plane and cross-plane conduction.

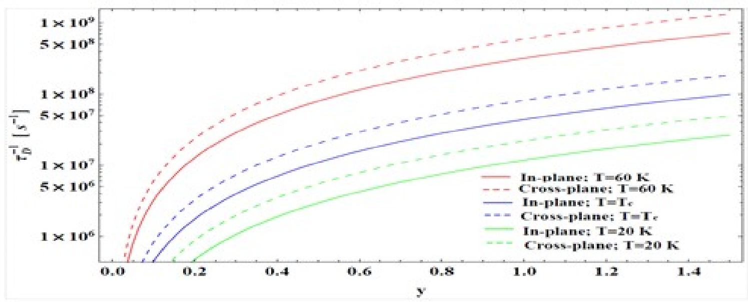

Figure-3: The variation of inverse relaxation time for defect scattering with reduced frequency (y = hω/k_BT) at different temperatures

3.1.3 for Phonon-Phonon Scattering

Apart from boundary and defect scattering, this scattering suggests that the trend for in-plane and cross-plane cases is similar but the thermal resistance offered by cross planes is certainly much higher than that for the in-plane, confirming a good degree of anisotropy in the material.

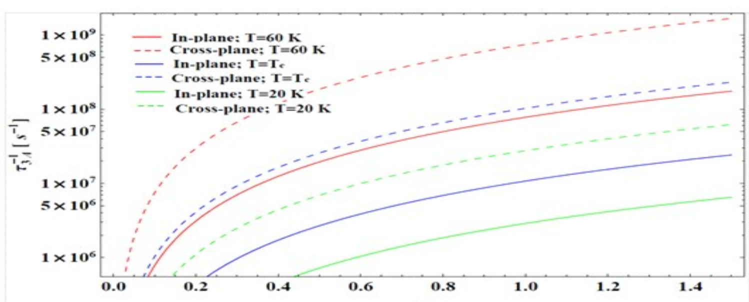

Figure:4- The variation of inverse relaxation time for phonon-phonon scattering with reduced frequency (y = hω/k_BT) at different temperature.

3.1.4 for Interference Scattering

For this scattering, the anisotropy or the in-plane and cross-plane transport is very small as the two curves are very close. Figure-5 shows the trends of inverse relaxation time for interference scattering with reduced frequency ($y = h\omega/k_BT$) at $T \leq T_c$; $T= T_c$ and $T \geq T_c$. As for other scattering processes also, the rate are much enhanced for higher temperatures, decreasing systematically as the temperature decreases.

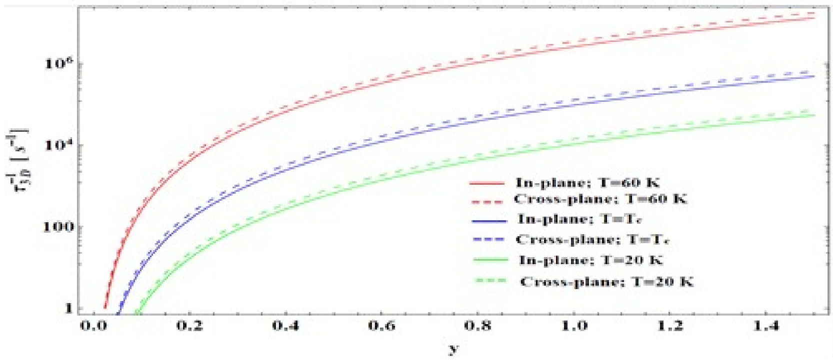

Figure-5: The variation of inverse relaxation time for Interference scattering with reduced frequency ($y = h\omega/k_BT$) at different temperature.

3.1.5 for Electron-Phonon Scattering

Electrons (i.e. carriers which in this case are holes) phonon scattering play a very important role in the thermal conduction in LSCO. The e-p scattering rate is weaker, in general, than that due to e.g. defects and interference terms, particularly for $T < T_c$. However, it picks up thereafter. This is due to carriers participating in pairon formation below Tc and increase in the pairon density as the temperature lowers. Electron-phonon interaction scattering events are highly sensitive to the phonon frequency variations (Figure-6) and help in understanding the fact that the pairons or superconducting Cooper pairs do not contribute to the thermal transport.

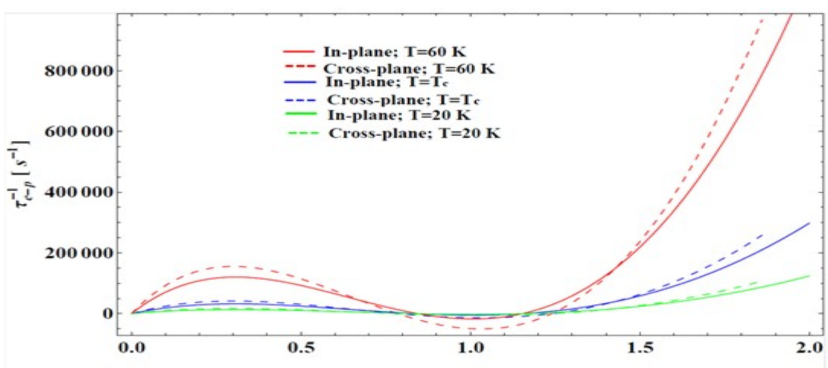

Figure-6: The variation of inverse relaxation time for electron-phonon (e-p) scattering with reduced frequency ($y = h\omega/k_BT$) at different temperatures.

The typical behavior of electron-phonon scattering events with reduced frequency ($y = h\omega/k_BT$) is shown in Figure-6, at $T < T_c$, $T = T_c$ and $T > T_c$. It is clear from the figure that below T_c, the electron-phonon scattering rate is very low due to the carriers participating in pairon formation not exchanging thermal energy with the phonons; in other words, such carriers (pairons) do not scatter the phonons. It also shows that the scattering rate, in general, stays low for the whole of the frequency range for $T < T_c$. This is applicable to even at $T= T_c$ to a good extent. As the temperature rises above T_c, the scattering rate shoots up (particularly for higher frequency phonons), since the carriers are now not bound in Cooper pairs and are able to efficiently exchange thermal energy with phonons.

3.1.6 for Resonance Scattering

The results indicate that the contribution of this term is almost the same for the in-plane and cross-plane thermal conduction. It's found that the moderate frequency phonons contribute to it, whereas the very low and high frequency phonons are almost non-contributing towards it. The resonance scattering process is found to be effective at relatively higher temperatures and the participating phonon frequencies also move to higher values with a rise in temperature (Figure-7). This term therefore is one of the scattering processes responsible for bringing about a dip in the thermal conductivity around or just below the $T_{c.}$

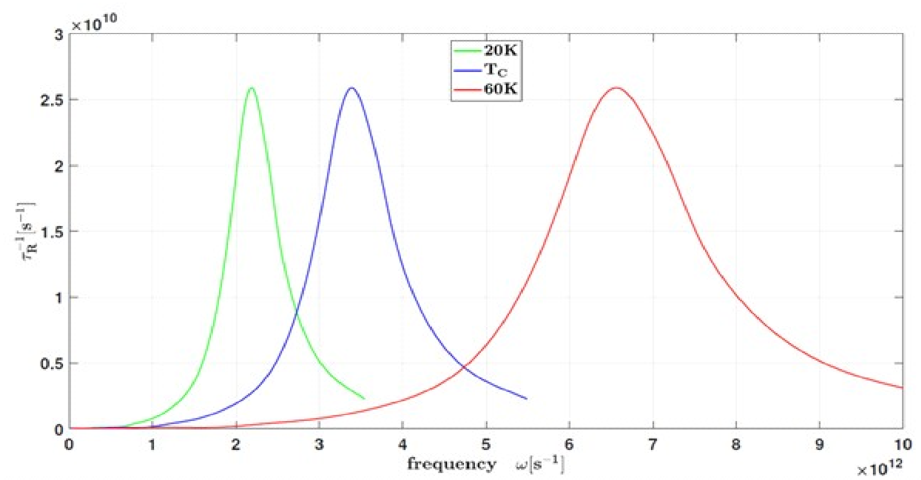

Figure-7: The variation of inverse relaxation time for resonance (R) scattering with reduced frequency ($y = h\omega/k_BT$) at different temperatures.

3.2. Thermal Conductivity for doped LCO

Next, the impact of Sr doping has been studied considering different doping concentrations 'x'. For x = 0.02, and 0.04, the LSCO is non-superconducting. For higher

https://doi.org/10.31995/voyager.2025.v16.015

concentrations x = 0.12, and 0.15, the material is superconducting with $T_c \sim 31$ K and ~ 37 K, respectively.

3.2.1 κ for Non-superconducting LSCO

The in-plane and cross-plane thermal conductivity has been numerically analysed for non-superconducting LSCO. The experimental results of Sun *et al.* [4], for the samples $La_{1.98}Sr_{0.02}CuO_4$ and $La_{1.96}Sr_{0.04}CuO_4$, have been employed for the temperature range 0-260 K. The sample dimensions are listed in Table-1. The numerical estimation has been carried out employing Equations 1 and 4. The calculated results along with the available experimental results have been portrayed in Figures 8 and 9. There is an excellent agreement between the calculated and experimental results throughout whole of the temperature range.

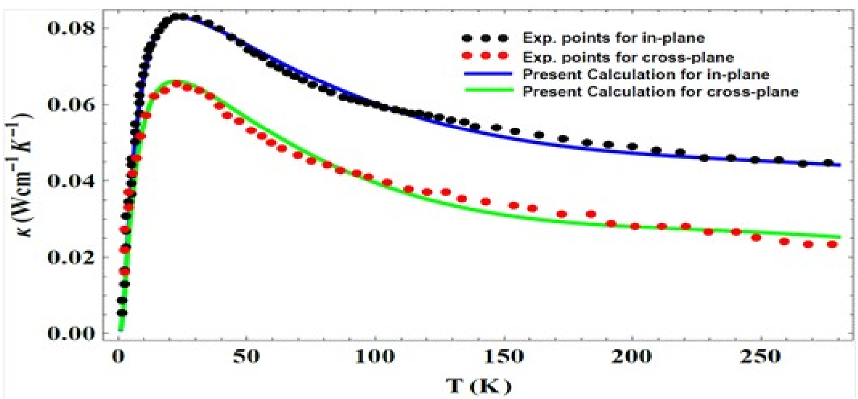

Figure-8: The temperature dependence of in-plane and cross-plane thermal conductivities of $La_{1.98}Sr_{0.02}CuO_4$.

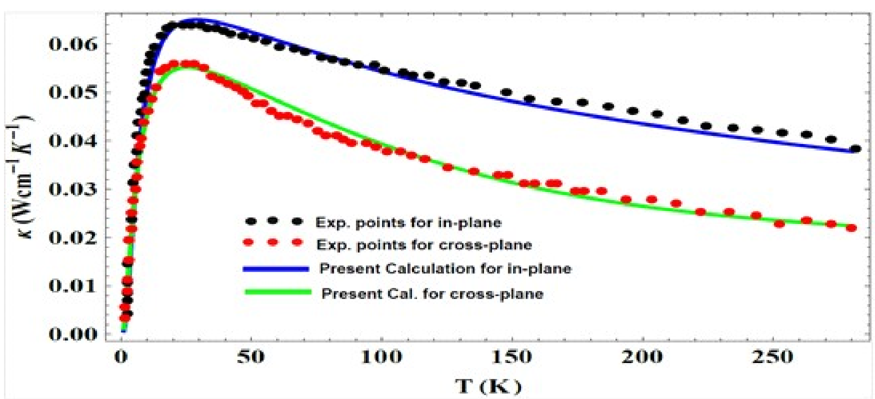

Figure-9: The temperature dependence of in-plane and cross-plane thermal conductivities of $La_{1.96}Sr_{0.04}CuO_4$.

Table-1: Parameters and coefficients used in the analysis of thermal conductivity of non-superconducting $La_{2-x}Sr_xCuO_4$ (x= 0.02 and 0.04).

		x = 0.02		x = 0.04	
Coefficient/parameter	Relates to	for K_{ab}	for K_c	for K_{ab}	for K_c
B(I) ($X10^{-3}$)	Boundary index	1.843	12.243	2.143	62.243
A ($X\ 10^{-42}\ s^3$)	Defect Scattering	5.012	11.911	7.882	8.921
B ($X\ 10^{-19}\ sK^{-1}$)	Multi-phonon Scattering	3.972	4.599	8.581	9.108
D ($X\ 10^{-45}\ s^3K^{-1}$)	Interference Scattering	3.214	15.842	0.114	1.314
A_{1e} ($X\ 10^2\ s^{-1}K^{-2}$)	Electron-phonon Scattering	7.482	7.980	7.482	7.980
A_{2e} ($X\ 10^2\ s^{-1}K^{-2}$)	Electron-phonon Scattering	7.581	7.878	7.482	7.980
R ($X\ 10^{31}\ s^2K^2$)	Resonance Scattering	0.457	1.571	0.501	0.557

On comparing with the thermal conductivity for the pristine material, it is noted that with doping of even the slightest amount of Sr, e.g. x=0.02, the magnon peak comes down dramatically (Figure -8) and becomes too broad to be conspicuous, even though the AFM order is still established at T_N = 240 K. For slightly higher Sr impurity concentration of x = 0.02, the high temperature peak totally fades away which is consistent with the fact that no Neel transition is observed for x = 0.02[4]. This clearly indicates that the Sr impurity is unfavourable to the magnon thermal transport. Various parameters used for the evaluation of k_{ab} and k_c for the non-superconducting LSCO are listed in Table-1.

3.2.2 κ for Superconducting LSCO

$La_{2-x}Sr_xCuO_4$ becomes superconducting as the doping level 'x' for Sr is increased beyond $x=0.05$. At the optimum doping of Sr at x= 0.15, this cuprate HTS $La_{2-x}Sr_xCuO_4$, has the maximum transition temperature of T_c ~ 37 K [4,9] (Figure-2). For superconducting LSCO (x = 0.12), the T_c is ~ 31$ K [20]. There are slight variations in the T_c values from different sources due to use of different approaches to determine the T_c e.g. for x = 0.12, the T_c is reported to be 29.2 to 31 K [11,20,21]. For x = 0.15, the T_c has been reported as 37 to 41 K [6,11,22].

The experimental data for k_{ab} and k_c are available for the doping x = 0.12 [4] and x = 0.15 [6]. Hence these two materials have been chosen for this study. Usually in superconducting materials, like YBCO, a peak is encountered in the K_{ab} on decreasing the temperature below T_c. It appears due to the formation of pairons (which, unlike the electrons, do not scatter the phonons) and opening up of the superconducting gap. However, LSCO for x = 0.12, shows a very inconspicuous and broad peak centered around the T_c.

For x = 0.15, there is a small dip around T_c which is present even for K_c.

Figure-10: The temperature dependence of in-plane and cross-plane thermal conductivities of $La_{1.88}Sr_{0.12}CuO_4$.

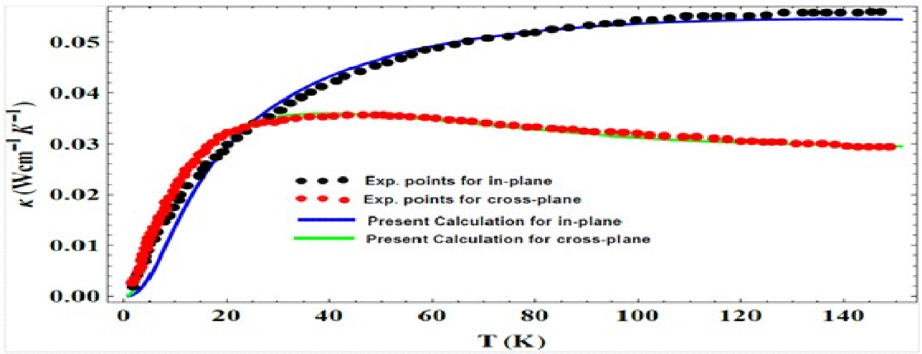

Figure-11: The temperature dependence of in-plane and cross-plane thermal conductivities of $La_{1.85}Sr_{0.15}CuO_4$.

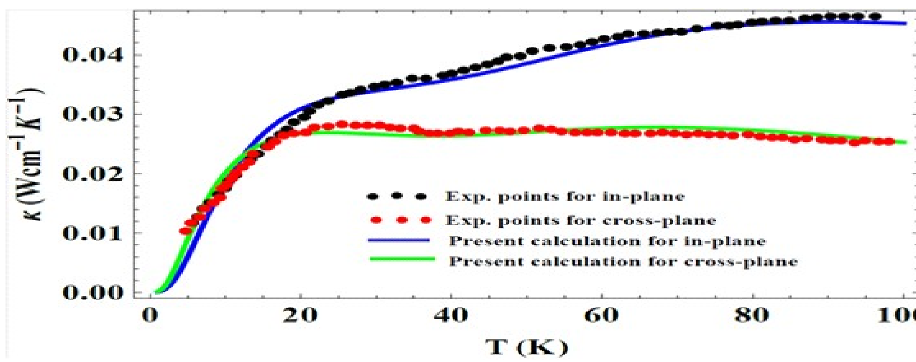

Table-2: Parameters and coefficients used in the analysis of thermal conductivity of non-superconducting $La_{2-x}Sr_xCuO_4$ (x= 0.12 and 0.15).

		x = 0.12		x = 0.15	
Coefficient/ parameter	Relates to	for K_{ab}	for K_c	for K_{ab}	for K_c
B(I) ($X10^{-3}$)	Boundary index	1.211	10.210	1.291	3.510
A ($X 10^{-42} s^3$)	Defect Scattering	9.421	9.982	7.521	9.127
B ($X 10^{-19} sK^{-1}$)	Multi-phonon Scattering	0.812	3.191	0.659	0.676
D ($X 10^{-45} s^3K^{-1}$)	Interference Scattering	0.0512	0.150	5.052	12.301
A_{1e} ($X 10^2 s^{-1}K^{-2}$)	Electron-phonon Scattering	8.890	8.981	8.482	8.980
A_{2e} ($X 10^2 s^{-1}K^{-2}$)	Electron-phonon Scattering	8.890	8.981	8.482	8.980
R ($X 10^{31} s^2K^2$)	Resonance Scattering	0.0312	0.041	1.022	0.110

During the numerical estimation of $La_{2-x}Sr_xCuO_4$ for x=0.12 and x=0.15, it is observed that the contribution of combined boundary and defect scattering events is highly effective at low temperatures but their significance gradually diminishes with the rise of temperature. Eventually the phonon-phonon scattering and interference scattering processes start leading. The values of various constants and parameters used in this analysis are furnished in Table-2, for each doping concentration. For superconducting LSCO for the in-plane and cross-plane conduction.

The phonon-phonon interactions and higher-order collision events indeed start dominating within the system when the temperature is continuously elevated. This results in the excitation of phonons of rising frequencies (i.e., of smaller and smaller wavelengths) facilitating the collisions at smaller distances. Thus, the thermal resistance continuously builds up, leading to a steady drop in the thermal conductivity.

The situation becomes so involved that the interference interactions start between the anharmonic phonon fields and the localized phonon fields giving rise to the scatterings, leading to stronger thermal resistance. This observation, that the multi-phonon and interference scattering processes dominate at and above the thermal conductivity maximum in the superconducting regime, is in consonance with earlier reports [15]. The electron-phonon interactions primarily participate in the thermal transport above the conductivity maximum in the case of high-temperature superconductors where, in general, the thermal conductivity curve shows a dip like trend near the transition temperature especially in the experimental data. This dip is more pronounced in the case of YBCO [14]. Since the pairons are generated as a result of phonon-mediated effects of electrons and do not contribute to the thermal transport, the onset of the superconducting phase (with lowering of the temperature) may be attributed to the negative thermal resistance (Figure-11) in this region, giving cusp-like behaviour at or around T_c. The various parameters used in computation are shown in Tables-1 and 2 infers that the in-plane values are always greater than those of cross-plane values.

3.3 Effect of Doping Concentration on Thermal Conductivity

To assess the effect of doping Sr in place of La, analysis of Figures 8 to 11 has been done. Looking at the comprehensive picture (Figure-12), it is observed that the magnitude of the maximum value attained by κ/T (at different temperatures) decreases continuously as the doping concentration 'x' increases. This indicates that the substitution of Sr for La acts as an impurity to effectively scatter the phonons. Even with 1% doping, a dramatic drop has been observed. The drop stretches even to the superconducting regime (x = 0.12 and 0.15). Throughout this range, the κ_{el} stays small and hence it is primarily the phononic thermal conduction that is affected adversely by Sr doping.

The phonon-magnon term's contribution in the parent compound LCO (an antiferromagnet with Neel temperature of ~ 270 K), which appears as a broad peak at ~270 K, is also affected drastically with even 2% doping of Sr, and the peak is hardly discernible in the thermal conductivity of $La_{1.98}Sr_{0.02}CuO_4$. Hence Sr doping also suppresses the antiferromagnetic ordering by introducing disorder at the Sr sites.

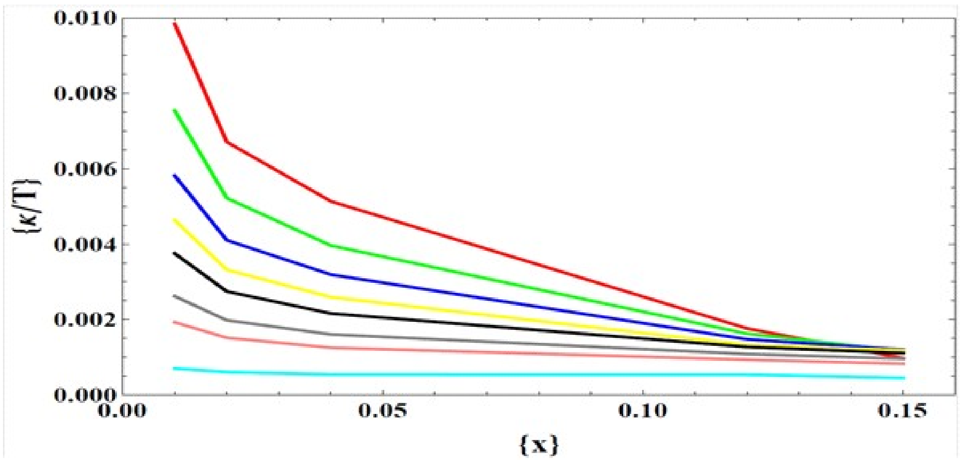

Figure-12: Doping dependence on thermal conductivity of $La_{2-x}Sr_xCuO_4$ at different temperatures.

4. Conclusions

The present chapter, dedicated to the study of thermal conductivity of single crystals of pristine and doped $La_{2-x}Sr_xCuO_4$ (x = 0.02, 0.04, 0.12 and 0.15) nicely explains the anisotropic behaviour of thermal conductivity. The steady drop in the magnitude of thermal conductivity as the Sr concentration increases clearly indicates that Sr impurity is detrimental to the thermal conduction in LCO.

Further, this study shows that for the doped compound, the thermal conductivity along the CuO_2 layers is always greater than in the direction perpendicular to these layers. This can be explained based on the stronger bonding in the $a-b$ plane (implying weak scattering of phonons, and hence a better thermal conduction) compared to weaker interlayer bonding (implying stronger scattering for thermal conduction along the '{c}' axis, hence a lower thermal conductivity). Contrary to this, the thermal conductivity for the pristine LCO shows a larger κ_c, compared to κ_{ab}. This can be understood by considering the AFM nature of LCO, hence phonon-magnon scattering also comes into play. The magnons are known to participate only in the CuO_2 plane dynamics. Hence the phonon-magnon scattering term influences (adversely) the in-plane thermal conductivity but doesn't affect the κ_c.

Consequently, for LCO the κ_c is larger than the κ_{ab}, which is opposite to what one has for the doped LCO where the AFM nature or the phonon-scattering term is ineffective or non-existent.

5. References

1. J. G Bednorz and K. A. Müller. (1986) Possible high Tc superconductivity in the Ba-La-Cu-O system. *Z. Physik B - Condensed Matter*, 64(2):189-193.
2. Gronborg, M. K., Lefmann, K. & Jacobsen, H. (2014). *"Growth and Characterization of LSCO Crystal"*, University of Copenhagen.
3. Uher, C. (1990). "Thermal conductivity of high-T_c superconductors", *Journal of Superconductivity* 3(4): 337–389.
4. Sun, X., Takeya, J., Komiya, S. & Ando, Y. (2003). " Thermal conductivities of lightly *Sr* and *Zn* doped La_2CuO_4 single crystals", *Physical Review B* 67(6): 104503.
5. D.T. Morelli, G.L. Doll, and J. Heremans.(1991) " Thermal conductivity of single-crystal lanthanum cuprates at very low temperature". *Solid State Communications*, 77(10):773-776.
6. Y. Nakamura, S. Uchida, T. Kimura, et al. (1991) "In-plane and out-plane thermal conductivity of La2-xSrxCuO4 single crystals ". *Physica C*, 185(189):1409_1410.
7. H. Ogasawara, M. Matsukawa, K. Noto, et al. (1994) "In-plane thermal conductivity of Ln2-xCexCuO4-y single crystals with the T-phase structure". *Physica C*, 235(240):1399_1400.
8. Poole, C. K., Farach, H. A. & Creswick, R. J. (1999a). *"Handbook of superconductivity"*, Elsevier.
9. Saxena, A. K. (2012). *"High-temperature superconductors"*, Vol. 125, Springer Science & Business Media.
10. S. Fujita and S. Godoy. (2001) *Theory of high-temperature superconductivity*, volume 121. Springer Science & Business Media.
11. Plakida, N. (2010). *"High-Temperature Cuprate Superconductors: Experiment, Theory, and Applications"*, Vol. 166, Springer Science & Business Media.
12. Fujita, S., Ito, K. & Godoy, S. (2009). "*Quantum theory of conducting matter: superconductivity"*, Springer Science and Business Media, New York.
13. Callaway, J. (1959). "Model for lattice thermal conductivity at low temperatures", *Physical Review* **113**(4): 1046–1051.
14. Kumari, A., Sharma, R., Chauhan, R., Indu, B. D. (2002). "The in-plane and cross-plane thermal conductivity of $RBa_2Cu_3O_{7-\delta}$ (R = Eu, Gd, Dy, Er) superconductors", *Physica scripta s* **94**: 065708.

https://doi.org/10.31995/voyager.2025.v16.015

15. V. Ashokan, B. D. Indu, and A. K. Dimri. (2011) Signature of electron-phonon interaction in high temperature superconductors. *AIP Adv.,* 1(3):032101.
16. V. Ashokan and B. D. Indu. (2013) Renormalization effects and phonon density of states in high-temperature superconductors. AIP Advances, 3(2):022108.
17. Singh, Anu, Singh, Hempal, Ashokan, Vinod, Indu, B. D.,(2013) Electrons and Phonons in High Temperature Superconductors, *Journal of Materials*, 2013, 605929, 4 pages.
18. A. Mourachkine. (2002) "High-Temperature Superconductivity in Cuprates". *Kluwer Academic Publisher*.
19. B. D. Indu. (1980) " Low-temperature lattice thermal conductivity of Mg2Sn, Mg2Si and Mg2Ge". *Il Nuovo Cimento B* (1971-1996), 58(2):345_350.
20. Z. X. Shen, A. Lanzara, S. Ishihara, and N. Nagaosa. (2002) Role of the electronphonon interaction in the strongly correlated cuprate superconductors. *Philos. Mag. B*, 82(13):1349_1368, 2002.
21. T. Kimura, K. Kishio, T. Kobayashi, Y. Nakayama, et al. (1992) "Compositional dependence of transport anisotropy in large (La, Sr)2CUO4 single crystals and second peak in magnetization curves". Physica C, 192:247_252.
22. K. Tanaka, T. Yoshida, A. Fujimori, D. H. Lu, Z. X. Shen, et al. (2004) "Effects of next-nearest-neighbor hopping t8 on the electronic structure of cuprate superconductors". Physical Review B, 70:092503.
23. Poole, C. K., Farach, H. A. & Creswick, R. J. (1999b). *Theory of high temperature superconductivity*, Kluwer.